Title	Second-harmonic generation in noncentrosymmetric phosphates
Author(s)	Li, Zhi; Liu, Qiong; Wang, Ying; Iitaka, Toshiaki; Su, Haibin; Tohyama, Takami; Yang, Zhihua; Pan, Shilie
Citation	Li, Z., Liu, Q., Wang, Y., Iitaka, T., Su, H., Tohyama, T., . . . Pan, S. (2017). Second-harmonic generation in noncentrosymmetric phosphates. Physical Review B, 96(3), 035205-. doi:10.1103/PhysRevB.96.035205
Date	2017
URL	http://hdl.handle.net/10220/46612
Rights	

Second-harmonic generation in noncentrosymmetric phosphates

Zhi Li,[1] Qiong Liu,[1,2] Ying Wang,[1] Toshiaki Iitaka,[3] Haibin Su,[4,5] Takami Tohyama,[6] Zhihua Yang,[1,*] and Shilie Pan[1,†]

[1]*Key Laboratory of Functional Materials and Devices for Special Environments of CAS, Xinjiang Technical Institute of Physics and Chemistry of CAS, Xinjiang Key Laboratory of Electronic Information Materials and Devices, 40-1 South Beijing Road, Urumqi 830011, China*

[2]*University of Chinese Academy of Sciences, Beijing 100049, China*

[3]*Computational Astrophysics Laboratory, RIKEN, 2-1 Hirosawa, Wako, Saitama 351-0198, Japan*

[4]*Division of Materials Science, Nanyang Technological University, 50 Nanyang Avenue 639798, Singapore*

[5]*Institute of Advanced Studies, Nanyang Technological University, 60 Nanyang View 639673, Singapore*

[6]*Department of Applied Physics, Tokyo University of Science, Katsushika, Tokyo 125-8585, Japan*

(Received 9 December 2016; revised manuscript received 6 July 2017; published 24 July 2017)

Motivated by the discovery of more and more phosphates with relatively strong nonlinear optic effect, we studied the mechanism of the second-harmonic generation (SHG) effect in several phosphates by band model and first-principles calculations. When the energy of an incident photon is much smaller than the band gap of material, the SHG is almost frequency independent and determined by the combination of Berry connection and a symmetric tensor. The SHG effect in phosphates can be enhanced by the enhancement of orbital hybridization or the reduction of charge-transfer energy, which results in widened bandwidth of occupied state and reduced band gap in the electronic structure, respectively. By the first-principles calculation on the electronic structures of several phosphates—BPO_4, $LiCs_2PO_4$, β-Li_3VO_4, and β-Li_3PO_4—we interpreted the relatively strong SHG effect in $LiCs_2PO_4$ and β-Li_3VO_4 as the consequence of the reduced charge-transfer energy compared to their parent β-Li_3PO_4, while the enhanced SHG in BPO_4 is resulting from enhanced orbital hybridization.

DOI: 10.1103/PhysRevB.96.035205

I. INTRODUCTION

Nonlinear optical (NLO) effects including second harmonic generation (SHG), photovoltaic effect, and nonlinear Kerr rotations have wide applications for the frequency conversion of laser light, solar cells, and optical devices, respectively [1,2]. NLO crystals for the SHG should have large band gap for high laser-induced damage threshold and moderate birefringence for phase matching. Currently, borate crystal $KBe_2BO_3F_2$ (KBBF) is widely used as NLO crystal because of its short ultraviolet (UV) cutoff wavelength ~150 nm, a moderate birefringence 0.077, and a relatively large SHG coefficient $d_{11} \sim 0.47$ pm/V [3]. However, the layered structure of KBBF reins its fabrication of single crystal with large size. Exploration for better NLO crystals is still an ongoing research topic in the material community.

NLO effect in phosphates with the PO_4 tetrahedron also has attracted research interest, with the exception of borates. As a typical phosphate, at low temperature Li_3PO_4 crystalizes into β structure with space group $Pmn2_1$, in which spatial inversion symmetry is absent [4]. Above 770 K, the β phase of Li_3PO_4 transforms into orthogonal structure with spatial inversion symmetry in which SHG is vanished. The SHG effect in β-Li_3PO_4 is very weak [5]. However, the SHG effect is observed in several materials as the derivatives of β-Li_3PO_4, such as β-Li_3VO_4, which has the same space group with β-Li_3PO_4 and presents very strong SHG $d_{24} = 10.2$ pm/V [6]. By $[KH_2]^{3+}$ substitution, KH_2PO_4 crystalizes into *I-42d* space group, and the SHG d_{36} of KH_2PO_4 is about 0.39 pm/V. Recently, two groups reported the relatively strong SHG d_{15}=d_{31} =-0.65 pm/V in the phosphate $LiCs_2PO_4$, which crystalizes into $Cmc2_1$ space group and has an optic band gap ~7.0 eV [7,8]. Although $LiCs_2PO_4$ and β-Li_3PO_4 have different space groups, they do share the same point group C_{2v}(mm2). The difference between space groups $Cmc2_1$ and $Pmn2_1$ is that the former has an additional lattice translation $T{:}(x,y,z) \longrightarrow (x+\frac{1}{2}, y+\frac{1}{2}, z)$, i.e., the latter is the subgroup of the former. Alternatively, the three Li atoms in the β phase of Li_3PO_4 can be substituted by one B atom, the synthesized BPO_4 crystalizes into tetragonal structure with $I\bar{4}$ ($S4$) space (point) group. BPO_4 has a short UV cutoff wavelength ~134 nm and a relatively large SHG $d_{36} = 0.76$ pm/V [9,10]. It is natural to ask what is the origin of relatively strong SHG in $LiCs_2PO_4$, β-Li_3VO_4, and BPO_4, which have the same valence number as β-Li_3PO_4, while the SHG in their parent β-Li_3PO_4 is very weak.

In the frame of single-particle physics, the NLO susceptibility can be calculated by the first-principles with the sum-over states (SOS) approximation [11–15]. However, it is difficult to identify the main contribution to NLO susceptibility because of many matrix elements and energy denominators. In the modern polarization theory, the charge polarization in periodic crystal is essentially connected with the Berry phase of Bloch wavefunctions [16–18]. Many interesting phenomena in condensed-matter physics, such as (anomalous) quantum Hall effect [19–24], are interpreted by the concepts of Berry connection and curvature within linear response theory. However, the interpretation of SHG in the view of Berry connection and curvature is still not fledged. The SHG is usually interpreted in the view of electric dipole (magnetic dipole) for nonmagnetic (magnetic) materials [25–30]. There are few works that attempt to understand SHG in the concept of Berry connection or curvature.

The Berry connection and curvature in momentum space read

$$\mathbf{a}_{nm}(\mathbf{k}) = i\langle u_n(\mathbf{k})|\nabla_{\mathbf{k}}|u_m(\mathbf{k})\rangle, \quad (1)$$

*zhyang@ms.xjb.ac.cn
†slpan@ms.xjb.ac.cn

and

$$\Omega_{nm} = \nabla \times \mathbf{a}_{nm}, \tag{2}$$

respectively, where $u_n(\mathbf{k})$ is a periodic part of the Bloch wave function, and n is the band index. Recently, from Boltzmann equation, Sodemann and Fu pointed out the nonlinear Hall effect in metallic system is related to the Berry curvature dipole (BCD) tensor $\mathbf{D}$ defined as [31]

$$D_{ab} = \frac{1}{(2\pi)^3}\int d^3k f_0(\partial_{k_a}\Omega_b), \tag{3}$$

in single band (omitting band indexes n and m) for the b component of the Berry curvature Ω_b, where f_0 is the electronic distribution at equilibrium (no perturbation). By the Floquet perturbation theory, Morimoto *et al.* proofed that the NLO conductivity tensor σ_{yxx} is also dependent on the BCD term $(2\pi)^{-3}\int d^3k\partial_{k_x}(\Omega_z)_{vv}$ [32,33],

$$(\Omega_z)_{vv} = -2\Im\frac{(v_x)_{vc}(v_y)_{cv}}{(\epsilon_v-\epsilon_c)^2}, \tag{4}$$

where $(v_x)_{vc} = \langle u_{v\mathbf{k}}|\partial_{k_x}h(\mathbf{k})|u_{c\mathbf{k}}\rangle$, with band index v (c) of occupied (unoccupied) states, and $h(\mathbf{k})$ is the unperturbed Hamiltonian in momentum space. Additionally, NLO response can also be adopted to measure the dynamical Berry curvature of metallic materials with time-reversal invariance (TRI) [34–37].

In this work, we started from a simple two-band model with weak orbital hybridization and large band gap. We proved that the Berry connection is increasing (decreasing) with the increasing orbital hybridization (charge-transfer energy). At the limit of low frequency, the transverse SHG is independent with frequency, which is completely different from the SHG at high frequency [38]. By first-principles calculation on the electronic structures of $LiCs_2PO_4$, β-Li_3PO_4, β-Li_3VO_4, and BPO_4, it reveals that the relatively strong SHG effect in BPO_4 is resulting from the enhanced sp orbital hybridization exclusively, while the relatively strong SHG in β-Li_3VO_4 and $LiCs_2PO_4$ results mainly from reduced charge-transfer energy. The calculated SHG by SOS approximation is consistent with experimental results qualitatively, and the flat part at low frequency also supports our results from band model calculation.

II. BAND MODEL

To interpret the role of the sp or dp orbital hybridization and charge-transfer energy, we construct an abstract model here. For a clear physics picture, we adopt a simple two-band model which has a general expression:

$$h(\mathbf{k}) = \begin{pmatrix} d_3(\mathbf{k}) & d_1(\mathbf{k}) - id_2(\mathbf{k}) \\ d_1(\mathbf{k}) + id_2(\mathbf{k}) & -d_3(\mathbf{k}) \end{pmatrix}. \tag{5}$$

Here, $d_3(\mathbf{k})$ is always positive, and off-diagonal term $d_1(\mathbf{k}) \pm id_2(\mathbf{k})$ is the hybridization between the two atomic orbitals. Vector $\mathbf{k}$ takes value in whole Brillouin zone (BZ). We drop term $d_0(\mathbf{k})$, because it just shifts the band energy globally and does not change the eigenvectors of the Hamiltonian $h(\mathbf{k})$. With regard to the nonmagnetic NLO crystals, the TRI is preserved while the spatial inversion symmetry is broken. The time-reversal symmetry T = K (conjugate operator) requires

$$h(-\mathbf{k}) = Th(\mathbf{k})T^\dagger, \tag{6}$$

i.e., both $d_1(\mathbf{k})$ and $d_3(\mathbf{k})$ are even functions of $\mathbf{k}$, while $d_2(\mathbf{k})$ is an odd function of momentum $\mathbf{k} = (k_x,k_y,k_z)$ in Brillouin zone. Without spin degree of freedom, the two atomic orbitals (bases) should have an angular momentum difference $\triangle m = \pm\hbar$, since the photon has momentum $\hbar$. If we chose the p orbitals as basis vector $(0,1)^T$, the basis vector $(1,0)^T$ should be s orbitals or d orbitals. The spatial inversion symmetry $P = \sigma_z$ (standard Pauli matrix) will further force $d_1(\mathbf{k}) = 0$. The eigenvalues of the Hamiltonian $h(\mathbf{k})$ read

$$\epsilon_{1,2}(\mathbf{k}) = \pm d(\mathbf{k}) = \pm\sqrt{d_1^2(\mathbf{k}) + d_2^2(\mathbf{k}) + d_3^2(\mathbf{k})}, \tag{7}$$

and the eigenvectors read

$$u_1(\mathbf{k}) = (\cos\alpha(\mathbf{k}), \sin\alpha(\mathbf{k})\exp(i\beta(\mathbf{k})))^T, \tag{8}$$

$$u_2(\mathbf{k}) = (-\sin\alpha(\mathbf{k})\exp(-i\beta(\mathbf{k})), \cos\alpha(\mathbf{k}))^T, \tag{9}$$

with

$$\cos\alpha(\mathbf{k}) = \frac{d(\mathbf{k}) + d_3(\mathbf{k})}{\sqrt{2d(\mathbf{k})[d(\mathbf{k}) + d_3(\mathbf{k})]}}, \tag{10}$$

$$\tan\beta(k) = \frac{d_2(\mathbf{k})}{d_1(\mathbf{k})}. \tag{11}$$

We should keep in mind that $\alpha(\mathbf{k})$ and $\beta(\mathbf{k})$ are even and odd functions of momentum $\mathbf{k}$, respectively. Because of $\cos\alpha(\mathbf{k}) \geqslant 1/\sqrt{2}$, $-\frac{\pi}{4} \leqslant \alpha(\mathbf{k}) \leqslant \frac{\pi}{4}$. The $\beta(\mathbf{k})$ satisfies $\beta(\mathbf{k}+2\pi) - \beta(\mathbf{k}) = \lambda 2\pi$, and λ is an integer, because of the periodicity of eigenvectors.

With the periodic part of Bloch wave functions $u_1(\mathbf{k})$ and $u_2(\mathbf{k})$, the Berry connections $\mathbf{a}(\mathbf{k})$ read

$$\mathbf{a}_{11}(\mathbf{k}) = -\sin^2\alpha(\mathbf{k})\nabla_{\mathbf{k}}\beta(\mathbf{k}), \tag{12}$$

$$\mathbf{a}_{12}(\mathbf{k}) = -(i\nabla_{\mathbf{k}}\alpha(\mathbf{k}) + s(\alpha)c(\beta)\nabla_{\mathbf{k}}\beta(k))e^{-i\beta(k)}, \tag{13}$$

$$\mathbf{a}_{21}(\mathbf{k}) = a_{12}^*(\mathbf{k}), \tag{14}$$

$$\mathbf{a}_{22}(\mathbf{k}) = -a_{11}(\mathbf{k}). \tag{15}$$

Here, $a_{11}(\mathbf{k})$ ($a_{12}(\mathbf{k})$) is intraband (interband) Berry connection. The real and imaginary parts of interband Berry connection $\mathbf{a}_{12}$ are even and odd functions of $\mathbf{k}$, respectively.

Starting from the SHG in the approximation of the electric dipole [1,2], we derived the SHG in periodic crystal with the conception of a Berry connection and position operator $\mathbf{r} = i\hbar\nabla_{\mathbf{k}}$ in periodic crystal [39]. Since we are interested with the off-resonant response, the complicated scattering terms are ignored [40]. Under a linear polarized optic field $E = E_x\exp(-i\omega t) + c.c.$, the transverse SHG effect $\chi^{(2)}$ along i direction of charge polarization reads (in atomic unit)

$$\chi^{(2)}_{ijj}(2\omega) = \frac{1}{(2\pi)^3}\int_{-\pi}^{\pi}\int_{-\pi}^{\pi}\int_{-\pi}^{\pi} d^3\mathbf{k}\Big\{\frac{(4\omega^2+2\omega_{ng}^2)a_j\Gamma_{ij}}{(4\omega^2-\omega_{ng}^2)(\omega^2-\omega_{ng}^2)} + \frac{a_i\Gamma_{jj}}{\omega^2-\omega_{ng}^2} + \frac{3\omega\omega_{ng}a_j\Omega_{ij}}{(4\omega^2-\omega_{ng}^2)(\omega^2-\omega_{ng}^2)}\Big\}, \tag{16}$$

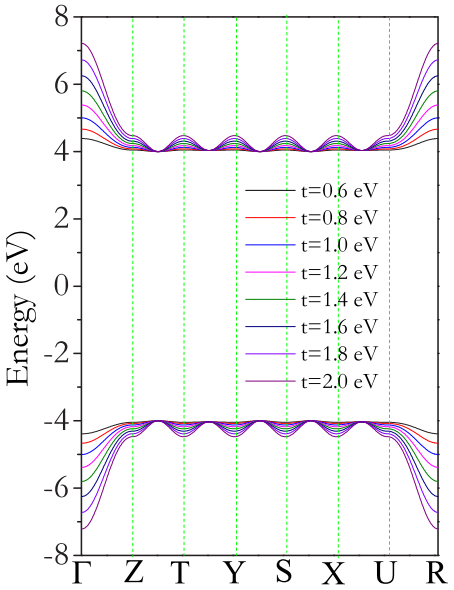

FIG. 1. Calculated band structures of two-band model with different hopping parameters.

where $a_i(\mathbf{k}) = i\langle g|\partial_i g\rangle = -i\langle n|\partial_i n\rangle$ is an intraband Berry connection that is an even function of $\mathbf{k}$ with $\partial_i = \partial_{k_i}$ and $|g\rangle$ ($|n\rangle$) being the periodic parts of Bloch functions for occupied (unoccupied) band indices, and

$$\Gamma_{ij}(\mathbf{k}) = \langle g|\partial_i n\rangle\langle n|\partial_j g\rangle + \langle g|\partial_j n\rangle\langle n|\partial_i g\rangle, \quad (17)$$

$$\Omega_{ij}(\mathbf{k}) = \langle g|\partial_i n\rangle\langle n|\partial_j g\rangle - \langle g|\partial_j n\rangle\langle n|\partial_i g\rangle. \quad (18)$$

The detailed derivation of Eq. (16) is presented in the Appendix. With TRI, the symmetric (antisymmetric) tensor Γ_{ij} (Ω_{ij}) is an even (odd) function of momentum $\mathbf{k}$, which is similar to the symmetric (antisymmetric) metric (curvature) tensor of two quantum states [41]. Since $a_i(\mathbf{k})$ is an even function of momentum $\mathbf{k}$, the terms including Ω_{ij} will vanish and not contribute to SHG. However, the term with Ω_{ij} is not vanished in system without TRI, even though the spatial inversion is preserved, i.e., magnetic material. In Eq. (16), the BCD term is absent since there is no correction on the position operator under external field, which is included in the Floquet band theory. The BCD term $\nabla_{\mathbf{k}}\Omega$, obtained from the Floquet band theory, is also an even function of momentum $\mathbf{k}$, and also can contribute to SHG in principles. However, large Berry curvature is usually associated with the band crossing or band inversion [42]. In our phosphates, there is no band crossing or inversion at all. This term should be very weak in our studied phosphates, though it is almost impossible to calculate it accurately because of lots of bands around Fermi level in the real material. However, if we further assume $\alpha(\mathbf{k})$ is constant, i.e., $\sqrt{d_1^2(\mathbf{k}) + d_2^2(\mathbf{k})}$ is constant in case of flat band, there is only one momentum $\mathbf{k}$ dependent function $\beta(\mathbf{k})$. In such a case, the Berry curvature dipole vanishes, while the symmetric metric-tensor-related terms still contribute to SHG. Additionally, since $\chi^{(2)} = \frac{\sigma^{(2)}}{2i\epsilon_0\omega}$ and BCD contributed $\sigma^{(2)} \propto \frac{1}{\omega}$, $\chi^{(2)}$ will diverge with $\frac{1}{\omega^2}$ at low frequency [32,33], it is obviously not reasonable in NLO materials studied here.

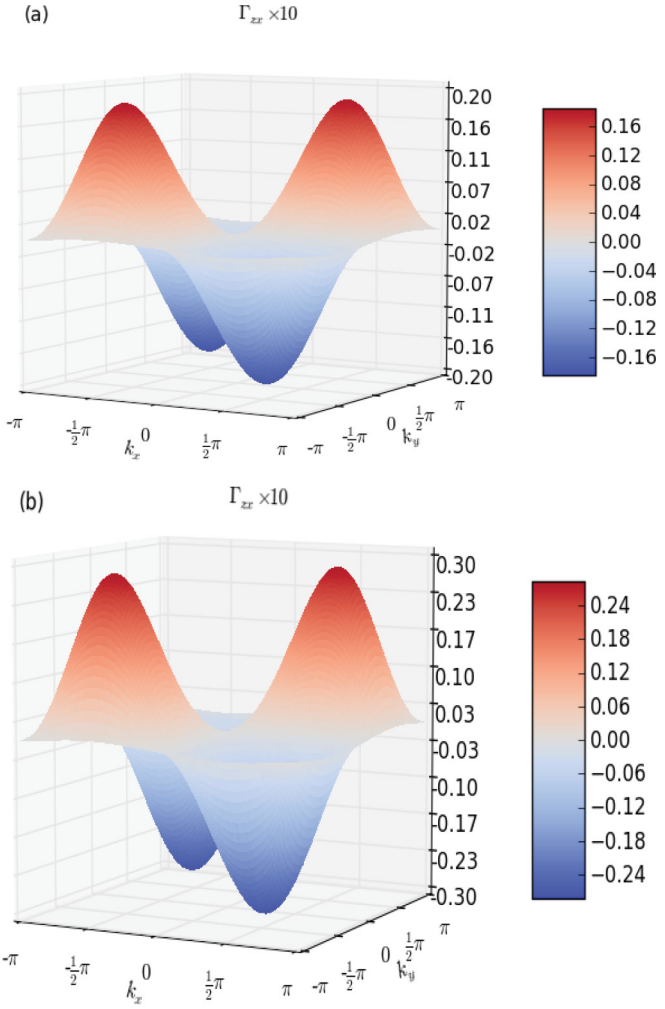

FIG. 2. The calculated Γ_{zx} on $k_y = 0$ plane with parameters $t_x = t_y = t_z = 0.8$ eV (a), and $t_x = t_y = t_z = 1.0$ eV (b).

With $d_1 = t_x \cos k_x + t_y \cos k_y + t_z \cos k_z$, $d_2 = \delta \sin k_z$, and $d_3 = 4.0$ eV, the two-band model Hamiltonian preserves the mm2 point group of β-Li_3PO_4 and β-Li_3VO_4, and the spatial inversion symmetry is broken by nonzero parameter δ. In real materials, the parameter δ is dependent on the orbital hybridization and deviation from centered position, and we adopt $\delta = 0.5$ eV in all studied materials here for simplification. Parameters $t_{i=\{x,y,z\}}$ are dependent on the hopping parameter, i.e, two-center integral of atomic orbitals ($sp\sigma$) or ($dp\sigma$) [43], and all $t_{i=\{x,y,z\}}$ are larger than δ. The bandwidth, defined as the difference of maximal and minimal eigenvalues of occupied state, is $\sqrt{d_3^2+(t_x+t_y+t_z)^2} - d_3$. With the increase of parameters t_x, t_y, and t_z, the bandwidth of occupied state is increasing, as shown in Fig. 1. The energy difference $2d(\mathbf{k})$ between the occupied and unoccupied bands also is increasing, except some momentum points on which $d_1(\mathbf{k}) = 0$.

At each momentum point $\mathbf{k}$, because of $\sin^2\alpha(\mathbf{k}) = \frac{d(\mathbf{k})-d_3(\mathbf{k})}{2d(\mathbf{k})}$ and $-\frac{\pi}{4} \leqslant \alpha(k) \leqslant \frac{\pi}{4}$, all intraband Berry connections $|\alpha(\mathbf{k})|$ and $|\sin\alpha(\mathbf{k})|$ are monotonically increasing with the enhancement of orbital hybridization strength $\sqrt{d_1(\mathbf{k}) + d_2(\mathbf{k})}$, which is increasing with the increase of any parameter t_x,t_y, or t_z. We calculated the Γ_{zx} tensor on $k_y = 0$

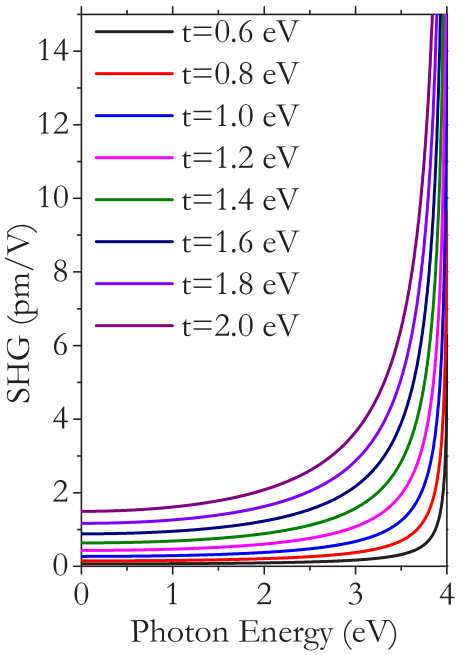

FIG. 3. The calculated photon energy dependent SHG $\chi^2(2\omega)_{zxx}$ with $t_x = t_y = t_z = t$.

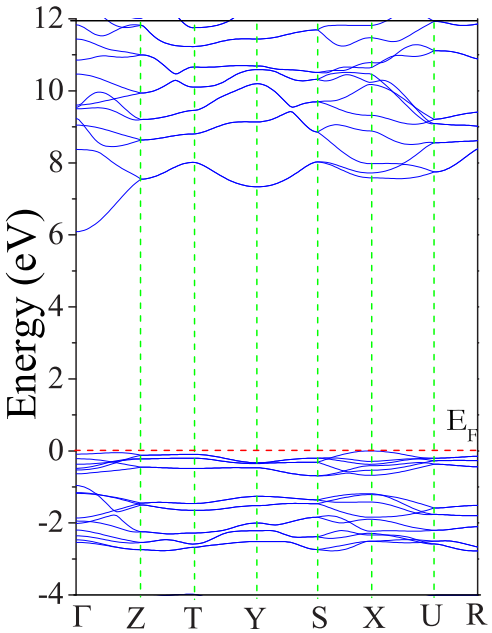

FIG. 4. Calculated band structure of β-Li_3PO_4 by first-principles calculation.

plane with parameters $t_x = t_y = t_z = t = 1.0$ and 0.8 eV. With these parameters, in fact, the Hamiltonian preserves a slightly higher point group, 4mm. As shown in Fig. 2, the calculated Γ_{zx} are even functions of momentum $\mathbf{k}$. The amplitude of Γ_{zx} is increasing with the increase of parameter t. The unit of Γ_{zx} is not specified, though it should be the square of length unit. The enhanced amplitude of Γ_{zx} can be interpreted by the enhancement of interband Berry connection resulting from increasing parameters $t_{i=\{x,y,z\}}$. Additionally, the amplitude of curvature tensor $\Omega_{zx}(\mathbf{k})$ is also increasing with the increase of parameter $t_{i=\{x,y,z\}}$, though it is an odd function of $\mathbf{k}$ and does not contribute to SHG here.

The calculated frequency dependent SHG from Eq. (16) is shown in Fig. 3, which indicated that SHG is also increasing with the increase of $t_{i=\{x,y,z\}}$.

Experimentally, we are interested in SHG at low frequency (say, 1064 nm wavelength), i.e., far before the double-photons resonance. From Eq. (16), we drop terms proportional to $(\frac{\omega}{\omega_{ng}})^n (n \geqslant 2)$, then the static SHG reads

$$\chi^{(2)}_{ijj} = \frac{1}{(2\pi)^3}\int_{-\pi}^{\pi}\int_{-\pi}^{\pi}\int_{-\pi}^{\pi} d^3k \left(\frac{a_i \Gamma_{jj}}{\omega_{ng}^2} + \frac{2\Gamma_{ij}a_j}{\omega_{ng}^2}\right). \quad (19)$$

With the concept of Berry connection and the help of TRS, the SHG formula in Eq. (16) is very concise. It indicates that the SHG is independent of the energy of the incident photon at static limit and only determined by the electronic structure of ground state. Compared to previous SHG formulas, including many position matrices [1,2,14], the different contributions to SHG here are classified by the parity of the tensor field associated with wave functions of ground state. The generalization of tensor field to many bands (or high dimension) is trivial.

We also note that all of the studied materials have very large band gap. The calculated band structure of β-Li_3PO_4 by first-principles calculation is shown in Fig. 4, which reveals that the band gap is about 6.0 eV and the band dispersion is minute. This band character indicates that d_3 should be much larger than hybridization parameters $t_{i=\{x,y,z\}}$. With $t_{i=\{x,y,z\}} \ll d_3$, the bandwidth of occupied state is $\frac{(t_x+t_y+t_z)^2}{2d_3}$, which indicates that bandwidth will be widened with the increase of hybridization parameters $t_{i=\{x,y,z\}}$. The band gap is $\sim 2d_3$, which is the same as the charge-transfer energy between the atomic orbitals. With further approximation $t_x = t_y = t_z = t$, and making use of

$$\sin^2\alpha(k) \sim \alpha^2(k) \sim \frac{t^2(\cos k_x + \cos k_y + \cos k_z)^2}{(2d_3)^2}, \quad (20)$$

both $\langle g|\partial_i n\rangle$ and Γ_{ij} are proportional to t^2 and

$$\chi^{(2)}_{ijj} \propto \frac{t^4}{(2d_3)^6}. \quad (21)$$

The significance of this expression is dual. On one hand, it indicates there are two approaches to enhance SHG, i.e., lower the charge-transfer energy or enhance the orbital hybridization. In real materials, we expect high SHG, while the large band gap is still preserved, so we have to reduce bond length to enhance the orbital hybridization, which can be realized by external pressure. On the other hand, band gap in our studied materials here is $\sim 2d_3$ and the bandwidth of occupied state is $\frac{(t_x+t_y+t_z)^2}{2d_3}$. There are some corresponding features in the electronic structure for enhanced SHG resulting from reduced charge-transfer energy or enhanced orbital hybridization. For reduced charge-transfer energy, the band gap should be reduced, while the bandwidth of valence band will be widened if the strong SHG is resulting from orbital hybridization. The bandwidth of valence band offers a simple method to estimate the SHG in NLO materials with large band gap (i.e., large charge-transfer energy). In real materials, parameters

$t_{i=\{x,y,z\}}$ are also different from each other. However, the main conclusion is still valid, except Eq. (21) is spoiled because of the combination of $t_{i=\{x,y,z\}} \cos k_i$. Our conclusion, i.e., strong Berry connection and SHG can be enhanced by orbital hybridization, is also valid even in NLO materials with any point group, only if the band characters of large band gap and minute dispersion are preserved.

III. ELECTRONIC STRUCTURES

In the previous section, we concluded that strong SHG is associated with the wide bandwidth of valence band or the reduction of band gap. In this section, we studied the electronic structures of β-Li_3PO_4, β-Li_3VO_4, $LiCs_2PO_4$, and BPO_4. Since Cs is a heavy element, the ion polarization is not responsible for the enhancement of SHG in $LiCs_2PO_4$ relative to its parent β-Li_3PO_4. We also calculated the ion polarization of BPO_4 under external field, and our calculated result reveals that the ion contribution is minute [44]. The studied phosphates here are also nonmagnetic, and spin polarization will not contribute to SHG. Since we also have no localized orbitals such as $3d$ and $4f$, which have strong electronic correlation, single-particle picture is enough here and, thus, SHG of phosphates should be related to their electronic structures. We calculated the electronic structures of β-Li_3PO_4, β-Li_3VO_4, $LiCs_2PO_4$, and BPO_4 by the first-principles calculation to elaborate the relatively strong SHG in $LiCs_2PO_4$, and β-Li_3VO_4, and BPO_4. The first-principles calculations based on density functional theory implemented in VASP were carried out within a primitive cell with $12 \times 12 \times 10$ ($16 \times 16 \times 16$) k-point grid for β-Li_3PO_4, β-Li_3VO_4, and $LiCs_2PO_4$ (BPO_4) [45]. The projector augmented wave pseudopotentials with Perdew, Burke, and Ernzerhof (PBE) exchange-correlation and 500 eV energy cutoff is used in our calculation [46,47]. The experimental lattice parameters from single crystal XRD are adopted.

The calculated partial density of state (DOS) of total s orbitals and p orbitals is shown in Figs. 5(a) and 5(b), respectively. It reveals that BPO_4 has the largest band gap, and $LiCs_2PO_4$ has the smallest band gap. In all the materials, the conduction bands and valence bands are mainly from the s orbitals and the p orbitals, respectively. Below the Fermi level, the partial DOS is mainly from the p orbitals of O. However, the partial DOS of s orbitals has some difference. The β-Li_3PO_4 has very low partial DOS from s orbitals of Li, while $LiCs_2PO_4$ has relatively high partial DOS from s orbitals of Li and Cs. We also note that the partial DOS from p orbitals distributes in a smaller energy range below Fermi level, while the partial DOS of p orbitals in β-Li_3PO_4 distributes in a larger energy range $[-3.0,0.0]$ eV. The shortest P-O bond lengths in $LiCs_2PO_4$ and β-Li_3PO_4 1.55 Å and 1.54 Å, respectively. The sp hybridization between P and O is weakened in $LiCs_2PO_4$ because of larger P-O bond length. The smaller band gap in $LiCs_2PO_4$ can be interpreted by the smaller charge-transfer energy between O $2p$ orbitals and Cs $6s$ orbitals. In contrast to the $2s$ orbitals of Li, the $6s$ orbitals of Cs is much more spatial extended. The sp hybridization between Cs $6s$ orbitals and O $2p$ orbitals (i.e., virtual p-s transition between O and Cs) can also contribute to SHG effect. By these facts in β-Li_3PO_4 and $LiCsPO_4$, the enhanced SHG effect should be related to reduction of charge-transfer energy between O $2p$ orbitals and Cs $6s$ orbitals, i.e, band gap.

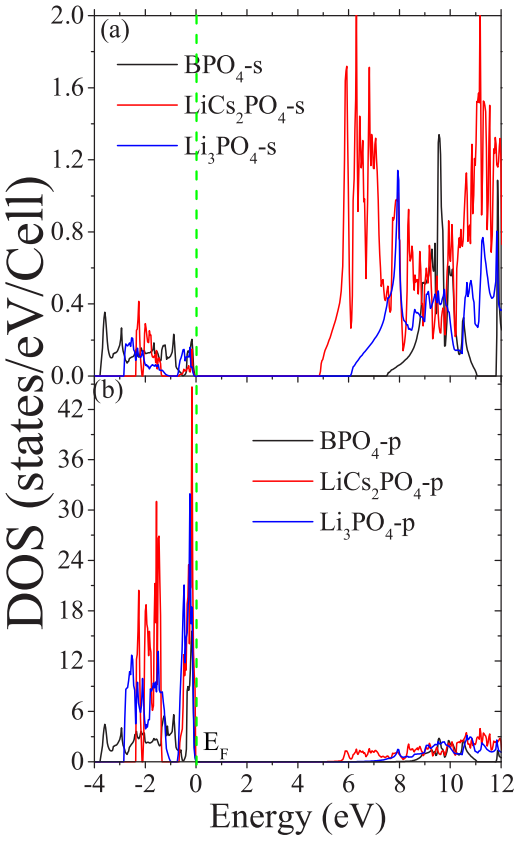

FIG. 5. The calculated partial DOS of (a)s orbitals and (b) p orbitals in β-Li_3PO_4, $LiCs_2PO_4$, and BPO_4.

Although BPO_4 also has low partial DOS from s orbitals of B, it has a similar SHG as large as that of $LiCs_2PO_4$. In these materials, the P-O bond length in BPO_4 is 1.53 Å, which is shorter than the P-O bond lengths in β-Li_3PO_4 and $LiCs_2PO_4$. In BPO_4, both the s orbitals from B and P contribute to the partial DOS above the Fermi level. With reduced P-O bond length, the sp hybridization between $3s$ of P and $2p$ orbitals of O will be enhanced. Strong sp hybridization will widen the bandwidth of valence bands. In the β-Li_3PO_4 parent, the sp is hybridized in the energy range $[-3.0,0.0]$ eV, while the bandwidth of BPO_4 is about 4.0 eV. The relatively large SHG effect can be interpreted by the strong sp hybridization exclusively.

Since the angular momentum difference between p orbitals and d orbitals is also $\hbar$, the P atom can be substituted by transition metals, such as V. The SHG effect of β-Li_3VO_4 is much stronger than those of BPO_4 and $LiCs_2PO_4$. The calculated DOS of β-Li_3VO_4 is shown in Fig. 6. It is obvious that the band gap of β-Li_3VO_4 is reduced seriously. The p orbitals of O and d orbitals of V also hybridize strongly in energy range $[-3.3,0.0]$ eV. The strong SHG effect can be interpreted by the combination of reduced charge-transfer energy and strong dp hybridization.

Overall, the characters in calculated DOS of studied materials here support our conclusion from the band model calculation, i.e., materials with relatively strong SHG effect

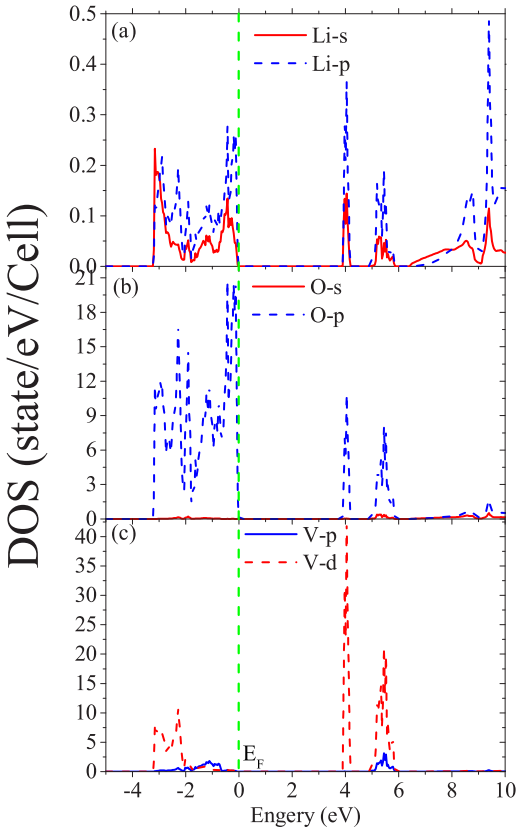

FIG. 6. Calculated partial DOS of Li (a), O (b), and V (c) in β-Li_3VO_4.

should have the electronic character of small charge-transfer energy between s orbitals (d orbitals) and p orbitals, or strong sp (dp) hybridization. In the DOS of electronic structure, BPO_4 has the largest band gap and bandwidth of p orbital dominating valence band resulting from strong sp hybridization, while the relatively strong SHG in β-Li_3VO_4 and $LiCs_2PO_4$ are mainly contributed by the reduction of charge-transfer energy. In the view of virtual transition, both strong orbital hybridization and relatively small charge transfer can enhance the electronic transition between s orbitals and p orbitals. In the studied phosphates here, the p-s transition between O-Cs compared to O-Li is stronger because of reduced charge-transfer energy, while the p-s transition between O-p in BPO_4 is enhanced by orbital hybridization resulting from shorter bond length, i.e., both O-P and O-Cs(Li) can contribute to SHG, and their weights to SHG are tunable by element substitution.

We also calculated the maximal SHG coefficients of β-Li_3PO_4, $LiCs_2PO_4$, and BPO_4 by the SOS approximation implemented in the ABINIT code [48,49]. In all studied materials here, the calculated band gap by modified Becke and Johnson local density approximation is larger than that calculated by PBE approximation by ~3.0 eV [44]. Because of the underestimated band gap by PBE approximation, a scissor operator 3.0 eV is used to enlarge band gap artificially in all calculations [50]. Since only hybridized bands contribute to SHG from our previous discussion, we only include the same number of conducting bands as valence bands in our calculation, i.e., total band number is the same as the electronic

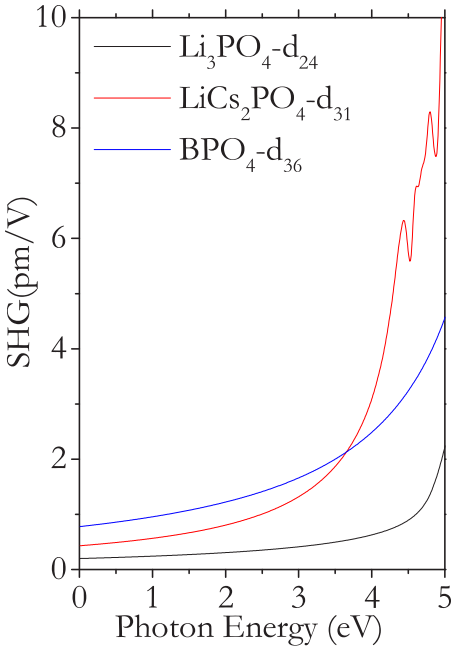

FIG. 7. Calculated SHG of β-Li_3PO_4, $LiCs_2PO_4$, and BPO_4 with SOS approximation.

number in primitive cell. The calculated results shown in Fig. 7 are consistent with experimental results qualitatively. The experimental SHG of BPO_4 ($LiCs_2PO_4$) under laser light with 1064 nm (i.e.,1.21 eV) are 0.76 pm/V (0.68 pm/V). For BPO_4 which has the largest band gap, the low frequency part of SHG within 0 ~ 2.0 eV is flat. For β-Li_3PO_4 and $LiCs_2PO_4$, the SHG is also very flat below 1.0 eV. This character of SHG at low frequency is consistent with our qualitative analysis in band model section, i.e., the low frequency part of SHG is mainly determined by the Berry connection and symmetric tensor of electronic structure. In the calculated SHG shown in Fig. 3, the low frequency part is also very flat. This consistency indicates the physics at low frequency is captured in the two-band model. However, near the double-photon resonance, the difference between model calculation and SOS approximation becomes obvious. Since only two bands are used, while the real materials have many bands, multiband effect becomes important near the double-photon resonance.

IV. SUMMARY

In summary, we studied the SHG of several typical phosphates by band model analysis in the view of Berry connection and first-principles calculation. By band model analysis, we concluded that the low frequency part of SHG should be determined by the Berry connection and a symmetric metric tensor. The SHG effect can be enhanced by the enhancement of orbital hybridization or the reduction of charge-transfer energy, which results in widened bandwidth of occupied state and reduced band gap in the electronic structure, respectively. By the first-principles calculation on the electronic structures of several phosphates—BPO_4, β-Li_3VO_4, $LiCs_2PO_4$, and β-Li_3PO_4—the relatively strong SHG effect in $LiCs_2PO_4$ and BPO_4 can be interpreted by the reduction of charge-transfer energy and the enhancement

of orbital hybridization, respectively, compared with their parent β-Li_3PO_4. The strong SHG in β-Li_3VO_4 is resulting from the combination of small charge-transfer energy and orbital hybridization. The calculated SHG effect by the SOS approximation is also consistent with the experimental results and the analysis from band model. The fundamental physics of SHG at low frequency limit is captured in the simple band model conclusion.

ACKNOWLEDGMENTS

This work is supported by the National Basic Research Program of China (Grant No. 2014CB648400), the National Natural Science Foundation of China (Grant No. 51425206),the Recruitment Program of Global Experts (1000 Talent Plan, Xinjiang Special Program), and the Director Foundation of XTIPC, CAS (Grant No. 2016RC001). T.T. and T.I. are supported by MEXT as "Exploratory Challenge on Post-K computer" (Frontiers of Basic Science: Challenging the Limits). The calculations were performed on the Hokusai system (Project Q17231, G17036) of Riken.

APPENDIX: SHG FORMULA IN LANGUAGE OF BERRY CONNECTIONS

In this appendix, we present the derivation of SHG formula in the language of Berry connection. Because of the large band gap and nearly flat band structures of our studied materials, we start the conventional SHG formula with dipole approximation [1,2]. The position operator $\mathbf{r}$ in insulator is $i\partial_{\mathbf{k}}$, and the charge polarization is the integral of a Berry connection of occupied band over the whole BZ. Because we are interested in the nonresonant response, we also ignore the relaxation from scattering. The SHG under external optic field with low frequency limit reads (in atomic unit).

$$\chi^{(2)}_{ijj}(2\omega)=\frac{1}{8\pi^3}\sum_{n,m,g}\int_{-\pi}^{\pi}\int_{-\pi}^{\pi}\int_{-\pi}^{\pi}d^3\mathbf{k}\left[\frac{\langle g|x_i|n\rangle\langle n|x_j|m\rangle\langle m|x_j|g\rangle}{(2\omega-\omega_{ng})(\omega-\omega_{ng})}+\frac{\langle g|x_j|n\rangle\langle n|x_j|m\rangle\langle m|x_i|g\rangle}{(2\omega+\omega_{ng})(\omega+\omega_{ng})}-\frac{\langle g|x_j|n\rangle\langle n|x_i|m\rangle\langle m|x_j|g\rangle}{(\omega+\omega_{ng})(\omega-\omega_{ng})}\right]. \tag{A1}$$

With $n=m\neq g$, the SHG reads

$$\chi^{(2)}_{ijj}(2\omega)=\frac{1}{8\pi^3}\sum_{n,g}\int_{-\pi}^{\pi}\int_{-\pi}^{\pi}\int_{-\pi}^{\pi}d^3\mathbf{k}\left[\langle n|x_i|n\rangle\left[\frac{A+iB}{(2\omega-\omega_{ng})(\omega-\omega_{ng})}+\frac{A-iB}{(2\omega+\omega_{ng})(\omega+\omega_{ng})}\right]-\frac{\langle n|x_i|n\rangle\langle g|x_j|n\rangle\langle n|x_j|g\rangle}{\omega^2-\omega^2_{nm}}\right]. \tag{A2}$$

where

$$2A=\langle g|x_j|n\rangle\langle n|x_i|g\rangle+\langle g|x_i|n\rangle\langle n|x_j|g\rangle, \tag{A3}$$

$$2iB=\langle g|x_j|n\rangle\langle n|x_i|g\rangle-\langle g|x_i|n\rangle\langle n|x_j|g\rangle. \tag{A4}$$

We sum all contributions from $n=m\neq g$, $n=g\neq m$, and $m=g\neq n$, by lengthy but straightforward calculation, the SHG reads

$$\begin{aligned}\chi^{(2)}_{ijj}(2\omega)=\frac{1}{8\pi^3}\sum_{n,g}\int_{-\pi}^{\pi}\int_{-\pi}^{\pi}\int_{-\pi}^{\pi}d^3\mathbf{k}\Bigg[&-2A\langle g|x_j|g\rangle\frac{4\omega^2+2\omega^2_{ng}}{(4\omega^2-\omega^2_{ng})(\omega^2-\omega^2_{ng})}\\&+\langle g|x_i|g\rangle\frac{2\langle g|x_j|n\rangle\langle n|x_j|g\rangle}{(\omega^2-\omega^2_{ng})}-2iB\langle g|x_j|g\rangle\frac{3\omega\omega_{ng}}{(4\omega^2-\omega^2_{ng})(\omega^2-\omega^2_{ng})}\Bigg].\end{aligned} \tag{A5}$$

Here, both valence band $|g\rangle$ and conducting band $|n\rangle$ are momentum $\mathbf{k}$ dependent. We redefine $-2A=\Gamma_{ij}$ and $-2iB=\Omega_{ij}$, then we get the Eq. (16) in main text.

[1] R. W. Boyd, *Nonlinear Optics*, 3rd ed. (Academic Press, Orlando, 2008).
[2] Y. R. Shen, *The Principle of Nonlinear Optics* (John Wiley and Sons, New York, 1984).
[3] L. Kang, S. Luo, H. Huang, T. Zheng, Z. S. Lin, and, C. T. Chen, J. Phys.: Condens. Matter **24**, 335503 (2012).
[4] A. R. West and F. P. Glasser, J. Solid State Chem. **4**, 20 (1972).
[5] S. Sakata, Y. Nagoshi, H. Nii, N. Ueda, and H. Kawazoe, J. Appl. Phys. **80**, 3668 (1996).
[6] S. Sakata and I. Fujii, Jpn. J. Appl. Phys. **30**, L1489 (1991).
[7] L. Li, Y. Wang, B.-H. Lei, S. Han, Z. Yang, K. R. Poeppelmeier, and S. Pan, J. Am. Chem. Soc. **138**, 9101 (2016).
[8] Y. Shen, Y. Yang, S. Zhao, B. Zhao, Z. Lin, C. Ji, L. Li, P. Fu, M. Hong, and J. Luo, Chem. Mater. **28**, 7110 (2016).

[9] X. Zhang, L. Wang, S. Zhang, G. Wang, S. Zhao, Y. Zhu, Y. Wu, and C. Chen, J. Opt. Soc. Am. B **28**, 2236 (2011).
[10] Z. Li, Z. Lin, Y. Wu, P. Fu, Z. Wang, and C. Chen, Chem. Mater. **16**, 2906 (2004).
[11] S. Sharma and C. Ambrosch-Draxl, Phys. Scr. **T109**, 128 (2004).
[12] J. L. P. Hughes and J. E. Sipe, Phys. Rev. B **53**, 10751 (1996).
[13] J. E. Sipe and E. Ghahramani, Phys. Rev. B **48**, 11705 (1993).
[14] J. E. Sipe and A. I. Shkrebtii, Phys. Rev. B **61**, 5337 (2000).
[15] C. Aversa and J. E. Sipe, Phys. Rev. B **52**, 14636 (1995).
[16] R. Resta, Rev. Mod. Phys. **66**, 899 (1994).
[17] R. Resta and D. Vanderbilt, *Physics of Ferroelectrics*,Vol 105, edited by C. H. Ahn, K. M. Rabe, and J. M. Triscone (Springer-Verlag, Heidelberg, 2007), pp. 31–68.
[18] D. Xiao, M.-C. Chang, and Q. Niu, Rev. Mod. Phys. **82**, 1959 (2010).
[19] X.-L. Qi, T. L. Hughes, and S.-C. Zhang, Phys. Rev. B **78**, 195424 (2008).
[20] N. Nagaosa, J. Sinova, S. Onoda, A. H. MacDonald, and N. P. Ong, Rev. Mod. Phys. **82**, 1539 (2010).
[21] E. Deyo, L. E. Golub, E. L. Ivchenko, and B. Spivak, arXiv:0904.1917.
[22] J. W. Mclver, D. Hsieh, H. Steinberg, P. Jarillo-Herrero, and N. Gedik, Nat. Nanotech. **7**, 96 (2011).
[23] P. Hosur, Phys. Rev. B **83**, 035309 (2011).
[24] H. Weng, R. Yu, X. Hu, X. Dai, and Z. Fang, Adv. Phys. **64**, 227 (2015).
[25] B. Koopmans, A.-M. Janner, H. T. Jonkman, G. A. Sawatzky, and F. van der Woude, Phys. Rev. Lett. **71**, 3569 (1993).
[26] G. Lefkidis and W. Hübner, Phys. Rev. Lett. **95**, 077401 (2005).
[27] T. Andersen, O. Keller, W. Hübner, and B. Johansson, Phys. Rev. A **70**, 043806 (2004).
[28] T. A. Luce, W. Hübner, A. Kirilyuk, Th. Rasing, and K. H. Bennemann, Phys. Rev. B **57**, 7377 (1998).
[29] A. Dähn, W. Hübner, and K. H. Bennemann, Phys. Rev. Lett. **77**, 3929 (1996).
[30] M. Fiebig, D. Fröhlich, Th. Lottermoser, V. V. Pavlov, R. V. Pisarev, and H. J. Weber, Phys. Rev. Lett. **87**, 137202 (2001).
[31] I. Sodemann and L. Fu, Phys. Rev. Lett. **115**, 216806 (2015).
[32] T. Morimoto, S. Zhong, J. Orenstein, and J. E. Moore, Phys. Rev. B **94**, 245121 (2016).
[33] T. Morimoto and N. Nagaosa, Sci. Adv. **2**, e1501524 (2016).
[34] J. E. Moore and J. Orenstein, Phys. Rev. Lett. **105**, 026805 (2010).
[35] K. S. Virk and J. E. Sipe, Phys. Rev. Lett. **107**, 120403 (2011).
[36] J. Wang, B.-F. Zhu, and R.-B. Liu, Phys. Rev. Lett. **104**, 256601 (2010).
[37] F. Yang and R.-B. Liu, Phys. Rev. B **90**, 245205 (2014).
[38] S. Scandolo and F. Bassani, Phys. Rev. B **51**, 6925 (1995).
[39] E. I. Blount, *Solid State Physics: Advances in Research and Applications*, Vol. 13 (Academic, New York, 1962).
[40] H. Haug, and Antti-Pekka Jauho, *Quantum Kinetics in Transport and Optics of Semiconductors* (Springer, Berlin and Heidelberg, 2008).
[41] M. Kolodrubetz, P. Mehta, and A. Polkovnikov, arXiv:1602.01062v2.
[42] Z. Fang, N. Nagaosa, K. S. Takahashi, A. Asamitsu, R. Mathieu, T. Ogasawara, H. Yamada, M. Kawasaki, Y. Tokura, and K. Terakura, Science **302**, 92 (2003).
[43] J. C. Slater and G. F. Koster, Phys. Rev. **94**, 1498 (1954).
[44] Z. Li, Q. Liu, S. Han, T. Iitaka, H. Su, T. Tohyama, H. Jiang, Y. Dong, B. Yang, F. Zhang, Z. Yang, and S. Pan, Phys. Rev. B **93**, 245125 (2016).
[45] G. Kresse and J. Hafner, Phys. Rev. B **47**, 558(R) (1993).
[46] G. Kresse and D. Joubert, Phys. Rev. B **59**, 1758 (1999).
[47] J. P. Perdew, K. Burke, and M. Ernzerhof, Phys. Rev. Lett. **77**, 3865 (1996).
[48] R. W. Nunes and X. Gonze, Phys. Rev. B **63**, 155107 (2001).
[49] X. Gonze, B. Amadon, P.-M. Anglade, J.-M. Beuken, F. Bottin, P. Boulanger, F. Bruneval, D. Caliste, R. Caracas, M. Cote, T. Deutsch, L. Genovese, Ph. Ghosez, M. G. S. Goedecker, D. R. Hamann, P. Hermet, F. Jollet, G. Jomard, S. Leroux, M. Mancini, S. Mazevet, M. J. T. Oliveira, G. Onida, Y. Pouillon, T. Rangel, G.-M. Rignanese, D. Sangalli, R. Shaltaf, M. Torrent, M. J. Verstraete, G. Zerah, and J. W. Zwanziger, Comput. Phys. Comm. **180**, 2582 (2009).
[50] F. Nastos, B. Olejnik, K. Schwarz, and J. E. Sipe, Phys. Rev. B **72**, 045223 (2005).